LAWRENCE LIVERMORE LABORATORY

University of California/Livermore, California

THERMO-OPTICAL LIMITATIONS ON HIGH AVERAGE POWER DYE LASERS

O. G. Peterson, A. A. Pease, and

W. M. Pearson

May 14, 1975

MASTER

THIS PAPER WAS PREPARED FOR SUBMISSION TO
1975 IEEE/OSA CONFERENCE ON LASER ENGINEERING AND APPLICATIONS
WASHINGTON, D.C., MAY 28-30, 1975

THERMO-OPTICAL LIMITATIONS ON HIGH AVERAGE POWER DYE LASERS*

O. G. Peterson, A. A. Pease, and
W. M. Pearson

Lawrence Livermore Laboratory
P. O. Box 808, Livermore, CA 94550
(415) 447-1100, Ext. 3327

The development of high average power, high repetition-rate dye lasers is vitally improtant in the evolution of commercially viable uranium isotope photoseparation processes.

There are many sub-areas of investigation that influence dye laser development; for incoherently pumped dye lasers, these include flashlamp studies dye and dye solvent optimization, and resonator configuration studies. Today, I will concentrate on what appears to be one of the more serious limitations to dye laser scaling -- thermo-optical limitations.

This slide (SLIDE #1) is a schematic of the laser head investigated. It consists of mutually orthogonal dye flow, pumping excitation, and laser output. There are three separate fluid flows in the head: low conductivity cooling water surrounding the flashlamps, water in the reflector head and the dye between the sapphire or quartz windows. The dye and head water were circulated through a heat exchanger to prevent systematic thermal gradients across the windows.

The dye employed in these investigations was coumarin 314: the flow rate through the head was 15 gal/min. For an active height of 3 mm, this resulted in a complete dye replacement every 3 msec. Thus, if no thermal effects other than dye heating were present, one would expect the energy per pulse of the laser to be level up to 300 Hz repetition rate, when portions of the same dye volume would be flashed twice. Tests revealed however (SLIDE #2)

that the turnover occurred much earlier. In this case, for quartz windows, the turnover occurs at about 100 Hz; for sapphire windows (SLIDE #3), whose thermal conductivity is somewhat greater than that of quartz, this turnover occurs at about 150 Hz.

Time resolved interferometry was chosen as the most sensitive probe of the active medium. A Michelson interferometer was assembled as shown in the next slide (SLIDE #4). The HeNe laser shown in conjunction with photo-diode #1 caused the command resonant charge apparatus to energize the capacitors. The argon laser, in conjunction with photo-diode #2 caused the capacitors to discharge,firing the flashlamps. Varying the wheel speed changed the flashlamp repetition rate. A single pulse from the chopped CW argon laser could be gated out with the mechanical shutter. This pulse, with photo-diode #3 fired the camera, as well as formed the interference fringes for observation. Relay optics were employed to present an image of the dye cell at the camera. Thus, any variation in optical pathlength through the dye cell would be seen as a fringe shift. Both the framing and streak options were employed with TRW camera. (SLIDE #5).

The upper 3 photographs are scope traces, all swept at 10 μs/division. In set (1) each spike in the upper trace indicates the time of each picture taken by the camera; the lower trace is the current pulse taken from a current viewing resistor at the flashlamps. The lamps were single pulsed for these pictures. Note the straight fringes in the first frame photograph in set (1). In the second and third frames of set (1) the fringes are distinctly curved,

indicating a thermally induced change in optical index of refraction
in the dye cell. Sets (2) and (3) are streak photographs of a similar
event with the slit located near the cell edge. The writing times in
relation to the current pulses are shown by the step trace here; a continu-
ous history of fringe motion is readily apparent in the photographs.
The flashlamp discharge visibly brightens the fringes. The displace-
ment of the fringes during the flashlamp pulse is caused by the change
in index due to the instantaneous temperature rise in the dye, the $\frac{\partial n}{\partial T}$
term in the equation in the middle of the slide. The continued fringe
displacement during and after the termination of the pulse is the
result of an index change due to density variations in the fluid, the
second term in the equation. These kinds of photographs will be employed
to evaluate the magnitude of these separate index variation terms.

On the assumption that thermal gradients of this type must be
responsible for the observed energy per pulse turnover, photographs
were taken to look for residual thermal gradients just prior to a pulse
at a variety of repetition rates. Photographs were taken at 15 second
intervals to determine the cumulative nature of thermal effects.

The first observable residual effects occurred at about 100 Hz
for the quartz windows and at about 150 Hz for the sapphire windows.
(SLIDE #6).

This slide depicts the type of data taken. This data was taken
with sapphire windows at 200 Hz flashlamp repetition rate. The oscillo-
graph in the upper left reveals the time relation of the photographs
with respect to the current pulse through the flashlamps. In the
upper right is a reference interferogram taken with the flashlamps

turned off. Each series of photographs were taken 2 μs apart with a
200 ns exposure. The residual thermal gradients remaining from the
previous flashlamp pulse become apparent upon comparison of the first
photograph in each trio with the reference. Steady-state conditions
are reached before 15 seconds in this case.

Enlargements of (a) and (b) in the slide (SLIDE #7) shows that the
residual thermal gradients cause a maximum half fringe variation over
the projected width of the cell. Thus, a plane wave incident on the
cell emerges with curvature. This curvature produced is equivalent
to that produced by a curved mirror of focal length f (SLIDE #8). For
a wavelength of 5145 Å and a projected cell half width of .856 mm, the
radius of curvature of the equivalent mirror is 5.7 meters. Since the
resonator employed in the tests was of the order of 1 meter long,
the effect of the curved mirror would produce a more stable, rather
than less stable, resonator.

(SLIDE #9) Closer examination of the photographs, however revealed
another effect. The effect, as shown in this slide is one of gross fringes
shift--an overall prism effect. Interferometrically this corresponds
to a rotation of a mirror in one of the legs. As may be inferred from
the interferogram, the initial alignment of the interferometer called
for a slight mirror rotation so that high order, closely spaced fringes
were projected through the dye cell. (SLIDE #10) The next slide depicts
conceptually the resonator in our experimental arrangement. The spacing
between fringes is x units, the angular spacing is α, Σ_1 and Σ_2 are the
two intersecting plane wavefronts, Σ_2 at the front mirror in the reso-
nator. The distance between points on the wavefront corresponds to
wavelength λ, which is equivalent to a shift of 1 fringe distance, x.

The calculation shows that a wavefront rotation of only .125 milli radian causes the same fringe displacement. Over a 1 m resonator, this amounts to a .125 mm displacement. It is reasonable to assume that this rotation is random in direction. Indeed our two photographs suggest that the prism effect had a vertical, as well as horizontal shift.
(Slide #11)

A .125 mm displacement per pass through a cell only 1.8 mm wide constitutes a serious loss mechanism, one which could be easily responsible for the observed energy/pulse turnover.

These experiments have demonstrated that the ultimate scalability of high power, high repetition rate dye lasers is currently limited by thermally induced prism-inhomogenieties. The exact nature of the spatial and temporal thermal propagation properties is presently being investigated through detailed computer modelling. A computer program has been written at LLL which solves for both transient and steady state temperature distributions in multidimensional systems. Even without modelling, however, it is obvious from the data that the thermal conductivity of the enclosing window material effects the ultimate performance of the laser.

A few potential solutions to this thermally induced prism effect come to mind. The first and easiest to implement is the use of a short, confocal resonator. These would permit higher repetition rates without energy per pulse degradations attributable to the prism effect. Their use, however, precludes the insertion of tuning elements into the resonator volume. A second generation solution might lie in **active**, between pulse, corrective measures.

Though the energy per pulse turned over at high repetition rates, the most promising of conclusions is that the interferometric studies reveal that the optical quality of the active medium remains good even at the highest flash repetition rates evaluated. This implies that with appropriate correction techniques very high average powers may be achieved.
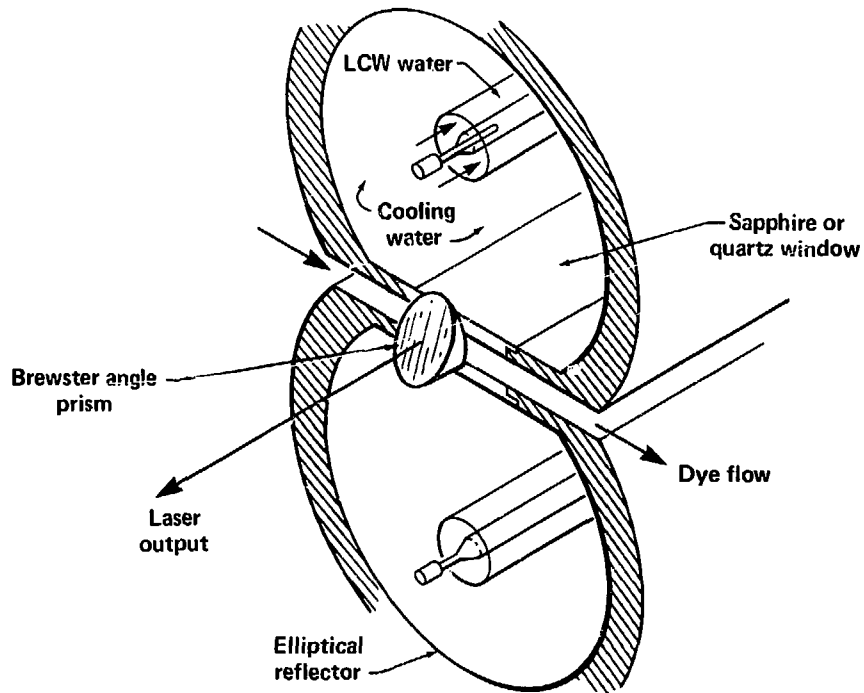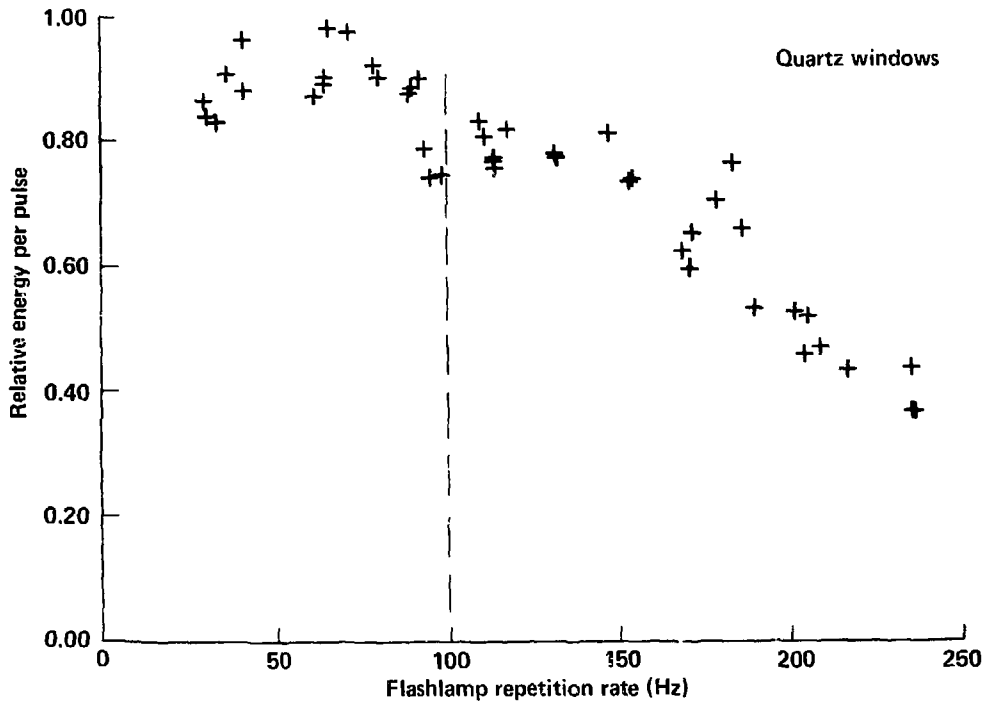
FIGURE 1

ENERGY PER PULSE vs FLASHLAMP REPETITION RATE
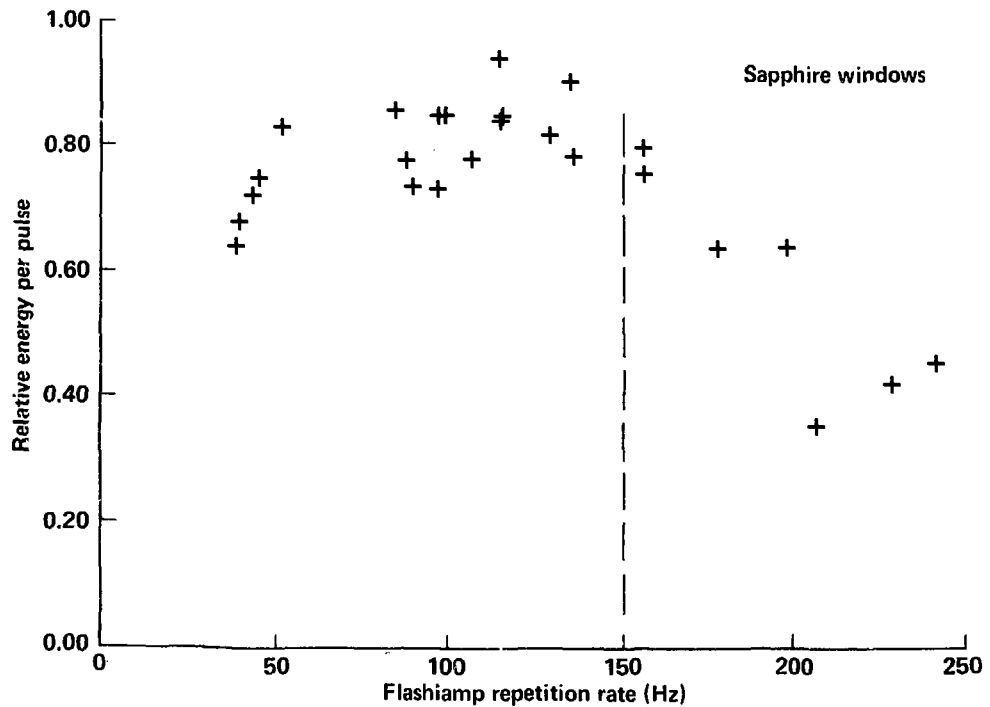
FIGURE 2
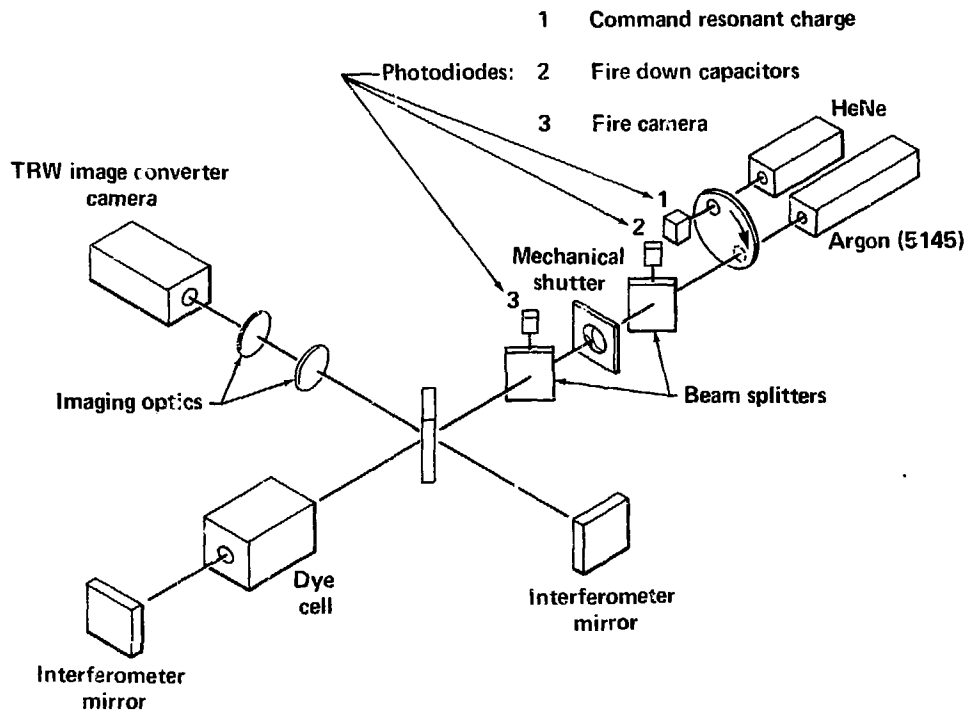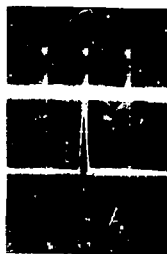
ENERGY PER PULSE vs FLASHLAMP REPETITION RATE

FIGURE 3

1   Command resonant charge

Photodiodes: 2   Fire down capacitors

3   Fire camera

HeNe

1

2

Argon (5145)

TRW image converter
camera

Mechanical
shutter

3

Imaging optics

Beam splitters

Dye
cell

Interferometer
mirror

Interferometer
mirror

FIGURE 4

10 μs/div

$$\frac{dn}{dT} = \frac{\partial n}{\partial T} + \frac{\partial n}{\partial \rho}\frac{\partial \rho}{\partial T}$$

10 μs between frames

200 ns exposure

Time

Reference

(1)

(2)

10 μs Write time

Time

Reference

(3)
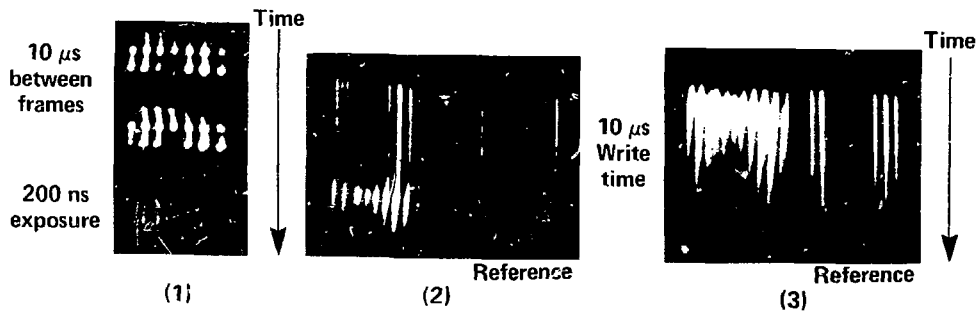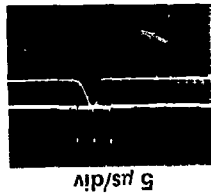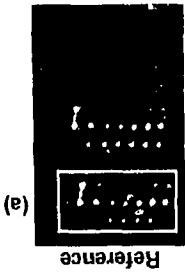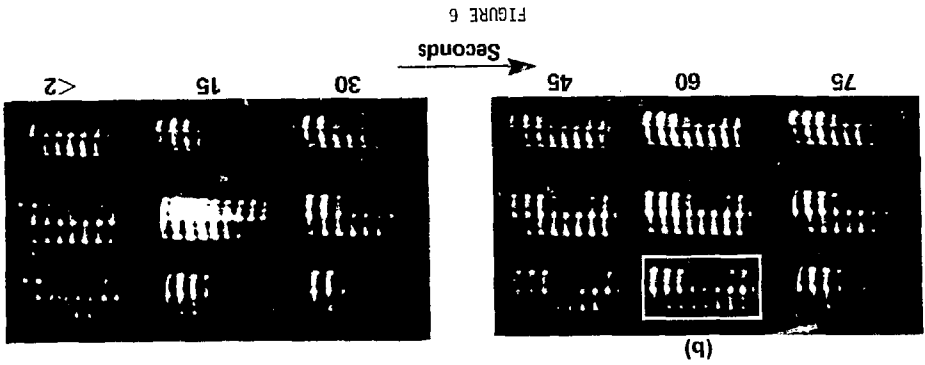
FIGURE 5

(a)
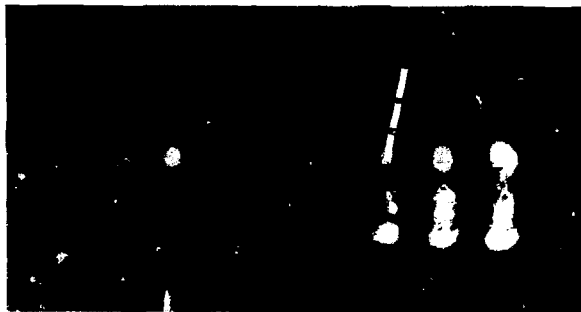
(b)
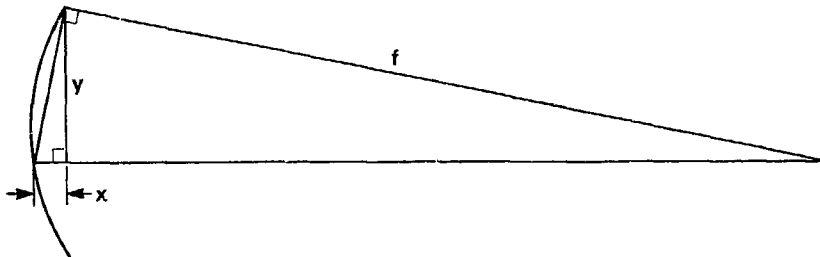
FIGURE 7

$$y = \frac{1.25\,\text{mm}}{n} = \frac{1.25}{1.46} = 0.856\,\text{mm projected}\ \frac{1}{2}\ \text{width}$$

$$x = \frac{5.145 \times 10^{-4}\,\text{mm}}{2}$$

$$\frac{f}{y} = \frac{y}{x} \qquad f = \frac{y^2}{x} = 2.84\,\text{m}$$

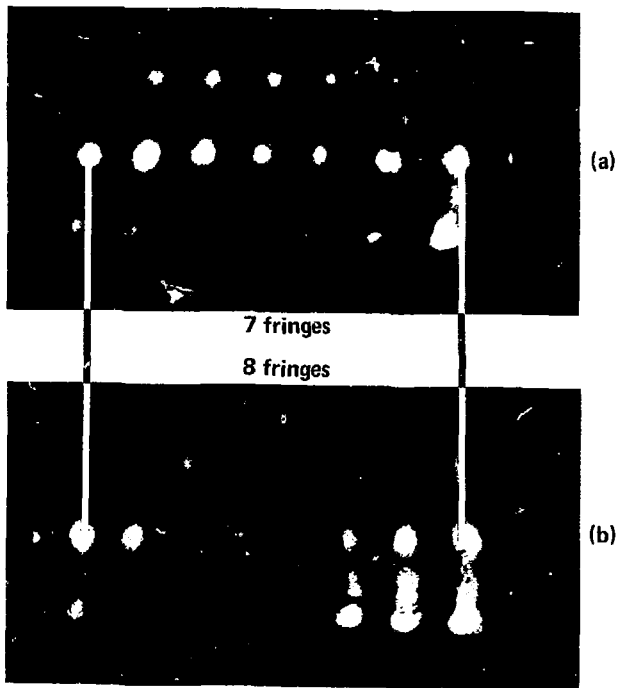**Radius of curvature ≈ 2f = 5.7 m**

FIGURE 8

7 fringes

8 fringes

FIGURE 9

$$\alpha = \frac{\lambda}{x}$$

$$d\alpha = -\frac{\lambda}{x}\frac{dx}{x}$$

$$x = 0.587 \text{ mm}$$
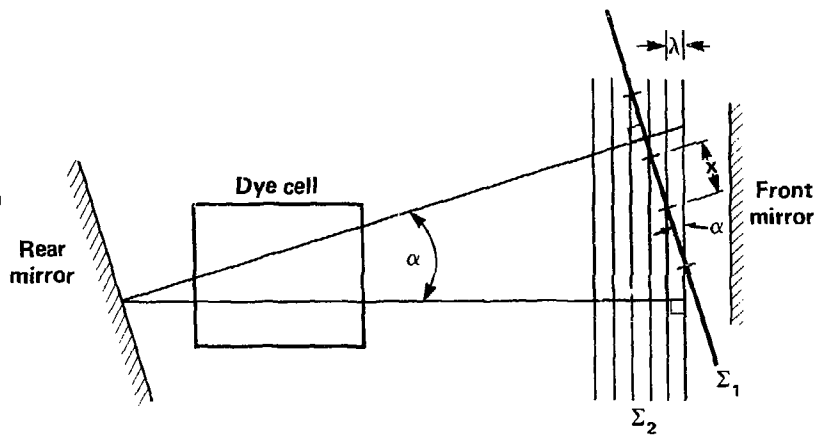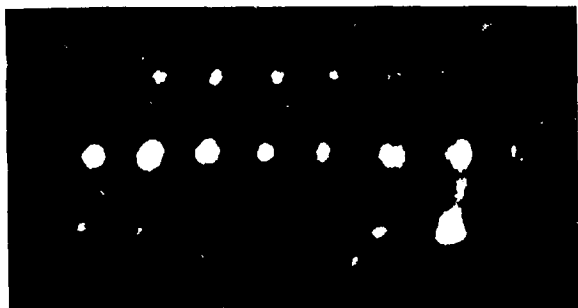
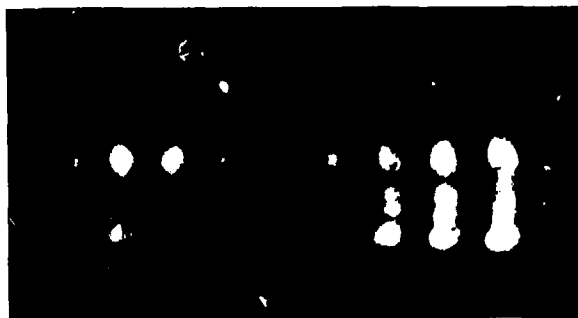$$\frac{dx}{x} = \frac{1}{7}$$

$$\lambda = 5145\text{Å}$$

$$\Delta\alpha = 0.125 \text{ mR}$$

FIGURE 10

(a)

(b)

FIGURE 11